buildings

MDPI

Article

Performance Evaluation of Hybrid One-Part Alkali Activated Materials (AAMs) for Concrete Structural Repair

Eddy Yusslee * and Sherif Beskhyroun

School of Future Environments, Auckland University of Technology, Auckland 1010, New Zealand
* Correspondence: eddy.yusslee@aut.ac.nz

Abstract: Alkali-activated materials (AAMs) have been widely used as an alternative to Portland cement. This production of AAMs emits lesser carbon dioxide by utilizing industrial waste products to make this cement binder technology greener and more sustainable. The conventional two-part system comprises solid aluminosilicate precursors with an alkali solution to activate the AAMs. However, higher alkalinity of the liquid activator is required to complete the geopolymerazation process, making the cementitious materials costly and sticky, and thus not convenient to handle on the construction site, affecting the worker's safety. A one-part AAMs system was introduced to overcome the two-part system's shortcomings. The alkali solution is now replaced with a solid alkali activator which is easier and more practical to apply at construction sites. This study was carried out to evaluate the mechanical performance of one-part alkali AAMs in the form of mortar by conducting compressive and flexural strength, modulus of elasticity, and tensile strength tests at 28 days of curing age under laboratory experiments in the tropical climate of Malaysia. A drying shrinkage test was also performed to detect its durability. Three types of solid admixtures were added to complete the composition of the novel mix design formulation. According to the results obtained, the mechanical strength of one-part alkali-activated mortar achieved the minimum requirement for Class R3 structural concrete repair materials as per EN1504-3 specifications. This eco-friendly cement binder has excellent potential for further engineering development, particularly to become a new concrete repair product in the future.

Keywords: fly ash (FA); ground granulated blast furnace slag (GGBFS); ordinary Portland cement (OPC); potassium carbonate; C-A-S-H

Citation: Yusslee, E.; Beskhyroun, S. Performance Evaluation of Hybrid One-Part Alkali Activated Materials (AAMs) for Concrete Structural Repair. *Buildings* **2022**, *12*, 2025. https://doi.org/10.3390/buildings12112025

Academic Editors: Zhihai He, Kunjie Fan, Dong Zhang and Nanting Yu

Received: 25 October 2022
Accepted: 17 November 2022
Published: 18 November 2022

1. Introduction

Alkali-activated materials (AAMs) have been widely used and regarded as a green technology mainly composed of industrial waste materials to reduce carbon dioxide (CO_2) emissions in the atmosphere. This technology was developed to reduce construction dependency on ordinary Portland cement (OPC). The OPC contributes to CO_2 emissions due to higher energy consumption and heat released from the calcination process [1]. In addition, many countries face deteriorated concrete structures as the building life spans approach their limit. This situation contributes to the higher demand for cementitious material to repair, refurbish, as well as reconstruct the buildings.

Furthermore, to keep the aesthetic value and heritage landmark for some buildings, many architects prefer those buildings to be refurbished to preserve them. As a result, sustainable building products are becoming popular among architects and engineers to ensure building elements can resist the load and keep maintenance costs minimum. Thus, the AAMs have become a substitute for conventional Portland cement, which has higher mechanical strength and more extended durability [2]. The conventional AAMs are prepared by two components, aluminosilicate precursor and alkali solution, to create an amorphous three-dimensional structure via the geopolymerization process. Common

aluminosilicate precursors used are alkaline by-products such as fly ash (FA), ground granulated blast furnace slag (GGBFS) and metakaolin (M) as alternative binders to replace OPC and produce a sustainable low-carbon cement material. Fly ash is an aluminosilicate product, mostly spherical particles but solid spheres and fines too, which react with $Ca(OH)_2$ to form gel products [3]. GGBFS is obtained when the iron is manufactured. It is generated in the blast furnace and then slaked. Lower silica and Na_2O modulus in GGBFS benefit higher hydration products due to the heat released [4]. Both FA and GGBFS are presented in powder form and have fine particle sizes beneficial for mechanical strength development. AAMs composed of FA or metakaolin will produce sodium aluminosilicate hydrate or N-A-S-H gels as the main reaction product, while AAMs composed of slag create calcium aluminosilicate hydrate or C-A-S-H gels, essential for cementitious binder materials [5]. In addition, FA and GGBFS have a higher content of amorphous phases favorable to accelerating the reaction scale for creating hardened products [6].

In addition, sodium hydroxide and sodium silicate are alkaline solutions frequently used to activate the precursors and form a hardened matrix comparable to OPC in a two-part AAMs system [7]. On the contrary, the two-part AAMs concept has setbacks in handling, mixing, and transportation issues besides heat curing requirements to achieve the required strength, making this product unsuitable for in situ construction [8]. Researchers introduce the innovative method of one-part alkali-activated materials as complementary to the traditional two-part concept. Aluminosilicate precursors are mixed with solid alkali activators to form a dry mixture, and water is added to initiate the geopolymerization process [9]. This 'just add water' method has improved AAMs properties in terms of mechanical strength, porosity, durability, and fast application, and it is easier to use. Kadhim et al. [10] explained the function of the alkali activator to provide an alkali medium and raise the pH for the reaction of mixtures by assisting the dissolution process of aluminosilicate precursors in AAMs technology. Four main alkali groups are commonly used to generate the hardened binder of this solid precursor: alkali hydroxide, alkali silicates, alkali carbonates, and alkali sulfates [11]. Anhydrous sodium metasilicate (Na_2SiO_3) is reported as the most suitable activator for the geopolymerization process but possesses a higher SiO_2/Na_2O ratio that makes it challenging to handle as such a corrosive chemical. For that reason, the lower SiO_2/Na_2O ratio of solid sodium carbonate is being studied as an alkali activator due to its low alkalinity level to provide safe and easy activator handling, compared to the sodium silicate activator or alkali hydroxide, which costs more and entails high CO_2 emission. On the contrary, besides its corrosivity, the total cost of sodium hydroxide is almost 5–6 times higher than the calcium oxide type of alkali activator. Hence, it is crucial to minimize the usage of alkali activators in AAMs and make this technology safe, practical, and cheap.

However, the investigation found that the one-part AAMs still have a low or inconsistent compressive strength, flexure strength, and shrinkage cracking [8,12]. Numerous studies have been conducted to improve the compressive strength of one-part AAMs, but most studies are limited to only the synthesis and characterization stage. As a result, the application of one-part AAMs technology in the form of mortar for concrete structural repair has still lagged. The class F fly ash (FA) is a low reactive precursor that was combined with calcium-rich slag to expedite the system's reactivity, subsequently abolishing the heat curing prerequisite, but it causes rapid hardening, which is not applicable for actual site application. A 15% slag reported was the optimum dosage of one-part AAMs mixed with 85% FA that improved the mechanical strength of one-part AAMs. Unfortunately, it was also activated with an 8% activator dosage that is still considered corrosive and costly [13]. Another study on one-part alkali-activated mortar composed of 40% GGBFS/60% FA and 10% anhydrous sodium metasilicate (Na_2SiO_3) showed higher compressive strength up to 80MPa but only managed to record 7MPa of flexural strength, less than 10% of its compressive strength [14], affecting its ability to resist bending for concrete repair application. The flexural strength (11 N/mm^2) and modulus of elasticity (27 GPa)

for mortar composed of 100% GGBFS were the highest compared to a single precursor of FA and metakaolin. Nevertheless, slag mortar could not bond vertically and horizontally, making it not applicable to concrete repair materials in the study conducted by [15]. The splitting tensile strength of up to 3.5–11 MPa for one-part alkali-activated mortar with the inclusion of fibre can be achieved, yet a higher alkali-activated dosage of between 8% and 10% is required to achieve that standard strength [8,16].

Including the OPC in AAMs mixtures can improve and accelerate the reaction rate for strength development [17]. Moreover, this type of mixed or blended cement is cheap. OPC is a type of hydraulic cement composed of hydraulic calcium silicates. This cementitious material creates calcium silicate hydrate or C-S-H gels as the main hydration products used as binding agents responsible for the strength. The combination of by-product precursor with the OPC can be activated by non-hygroscopic alkali, which is beneficial in preventing the inclination for efflorescence, high permeability, and more severe water absorption problems. A 60% OPC added in one-part AAMs concrete recorded 55.0 N/mm^2 compressive strength at 28 days of age provides essential information in designing one-part AAMs in the form of mortar for patching concrete repair techniques. This concrete consists of coarse aggregate and has also been activated with a significantly higher 12% potassium carbonate [18].

Furthermore, the inclusion of 15% waste concrete fines was reported to improve the mechanical strength of AAMs. Still, excessive waste construction (concrete) fines adversely impact the mechanical strength due to slow hydration degree and insufficient high calcium content, reducing C-A-S-H gels [19]. In addition, the recycled concrete powder also increases porosity in two-part AAMs due to low polymerization activity, creating a more porous microstructure [20].

The larger shrinkage level of AAMs was also the primary concern in both two-part and one-part systems. Hence, the presence of shrinkage-reducing admixtures (SRA) and calcium oxide (CaO) could control the expansion of hardened AAMs [21]. Moreover, combining SRA and CaO can stabilize the shrinkage effect [22]. A higher concentration of alkali activator may assist the degree of hydration, but higher heat release creates more expressive shrinkage after drying [23]. Adding CaO, which can provide extra alkalinity and calcium sources for forming C-S-H gels from the cement binder, can reduce reliance on the alkali activator and increase the mechanical strength. This is in agreement with the fact that strength development is reduced when calcium content decreases [24]. Still, excessive contents of both SRA and expansive additive of CaO may cause other side effects, such as fast setting and losses of water or moisture, and thus be ineffective in reducing drying shrinkage level [25]. To control the fast setting problems, a lignosulfonate-based superplasticizer (SP) was used to regulate the setting time of high calcium one-part AAMs and avoid setting too quickly, which is essential for transporting fresh materials from batching plant to the site [26]. The previous study on the potential admixtures for one-part alkali-activated materials (AAMs) also suggested that by adding SP to the mixtures, the water content can be optimized to improve the compressive strength of the mortar [27].

Therefore, this experiment's objective is to evaluate the mechanical strength performance of one-part alkali-activated mortar composed of different dosages of aluminosilicate precursors and activated with low dosages of solid alkali activators for concrete structural repair applications. The main precursor source used in this study was composed of the industrial by-product of fly ash (FA) and ground granulated blast furnace slag (GGBFS) combined with ordinary Portland cement (OPC), unlike typical one-part AAMs which are commonly composed of by-products powder only. Potassium carbonate (K_2CO_3) is a single solid alkali activator used to activate the precursors and as the source of alkali besides the existing sodium and potassium element (Na_2O and K_2O) in the OPC itself. In addition, three powder admixtures were added and tested to stabilize the hardened material's physical properties. Furthermore, a test for drying shrinkage level for durability was also carried out. To the author's knowledge, no previous studies were

conducted to evaluate the potential of one-part alkali-activated mortar composed of hybrid precursors and activated with a low alkaline solid alkali activator used for concrete structural repair application as an alternative to the conventional two-part AAMs system.

This study aims to comply with the compressive strength requirement with Class R3–EN1504 standard for structural concrete repair materials. According to the EN1504 standard, for non-structural concrete repair materials Class R2, compressive strength must be above 15 N/mm^2. For structural concrete repair, Class R3 ≥ 25 N/mm^2 and ≥ 45 N/mm^2 for Class R4 [28]. The novel mix design formulation reported in this study is vital for the author's continued research on utilizing one-part AAMS technology for green and sustainable building products. The experiment was conducted in Kuala Lumpur, Malaysia, a country with a tropical climate which is hot and humid throughout the year.

2. Materials and Methods

Class F fly ash (FA) and ground granulated blast furnace slag (GGBFS) were used as precursors under ASTM C618 and ASTM C989, respectively. Ordinary Portland cement (OPC) was added as the primary binder source and activated with alkali-activated powder-potassium carbonate (K_2CO_3 Purity ≥ 90%). The chemical compositions and physical properties of all main precursors are shown in Table 1. Natural sand was used as fine aggregate with a specific gravity of 2.67 and an average particle size of 90.23 μm (D50). In addition, a commercial ethylene glycol type shrinkage-reducing admixture (SRA) and calcium oxide (CaO) were added as an admixture in the form of solid powder. At the same time, the sodium lignosulfonate powder-based superplasticizer (SP) was also used in the experiment as a retarder for the mortar samples.

Table 1. Chemical compositions (%) and physical properties of Fly Ash (FA), Ground Granulated Blast Furnace Slag (GGBFS) and ordinary Portland cement (OPC) were obtained from the manufacturer.

Chemical Compositions	FA (%)	GGBFS (%)	OPC (%)
SiO_2	55.94	35.91	23.97
Al_2O_3	22.60	16.56	5.27
Fe_2O_3	8.10	1.52	3.28
CaO	6.26	35.28	60.12
P_2O_5	0.36	0.36	-
MgO	1.21	6.01	1.36
K_2O	1.66	-	0.51
TiO_2	0.72	0.59	0.06
SO_3	1.02	0.36	2.20
Na_2O	0.62	1.76	0.23
CI	0.03	-	-
LOI	1.48	-	2.00
Physical Properties			
Specific Gravity	2.20	2.90	3.15
Average Particle Size (D50)	14.08 μm	19.99 μm	16.32 μm

2.1. Mix Proportions

The experimental study was conducted to understand the effect of aluminosilicate precursors with different volume ratios, with OPC as the main binder and activated with a low percentage of alkali-activated powder. Besides that, three powder-type admixtures were added to all mixtures to investigate the effect of these admixtures compared to the samples prepared without admixtures. There were three stages of the experiment. All the samples were marked as Mix 1 to Mix 30 and consisted of FA, GGBFS, and with/without OPC as main precursors with different volume percentages. Stage 1, Mix 1, was chosen as

a control sample no.1, where the mixture contained only FA and GGBFS without OPC. For the second stage, Mix 10 was prepared as control sample no.2, which contained no admixtures. At the third stage, Mix 26 was chosen as control sample no.3 based on the findings on mechanical strength results for Mix 16–25 at 7 days of age (within the second stage experiment). The admixtures proportion for every sample was added into the mortar samples between 1.0 to 15.0 wt% of weight (based on total aluminosilicate precursors weight). The water-to-binder ratio was set between 0.30 to 0.50, and the aggregate-to-binder ratio was between 1 and 3 to produce the mortar, tested in all 30 mortar mixture samples and cured under the lab ambient conditions. The mix design compositions of one-part alkali-activated mortars are further elucidated in Table 2.

Table 2. Mix composition and design of one-part Alkali Activated Materials (AAMs).

Samples	Binder			Alkali Activated	Admixtures			Design Ratio	
	FA (%)	GGBFS (%)	OPC (%)	K_2CO_3 (%)	SRA (%)	CaO (%)	SP (%)	Aggregate-to-Binder	Water-to-Binder (W/B)
* Mix 1	85	15	0	6	5	1	1	3	0.30
Mix 2	25.5	4.5	70	6	1	0.5	1.5	3	0.30
Mix 3	60	10	30	6	5	1	1	3	0.35
Mix 4	59.5	10.5	30	6	5	1	1	1.5	0.46
Mix 5	25	5	70	6	2	1	1	1	0.49
Mix 6	45	5	50	5	2	1	1	1.5	0.45
Mix 7	59.5	10.5	30	6	5	1	1	1	0.35
Mix 8	81	9	10	6	4	1	1	1	0.35
Mix 9	60	10	30	6	5	1	1	1	0.35
** Mix 10	60	10	30	6	-	-	-	1	0.35
Mix 11	60	10	30	6	4	1	1	1	0.35
Mix 12	60	10	30	8	4	10	1	1	0.35
Mix 13	60	10	30	10	5	15	1	1	0.40
Mix 14	45	5	50	8	4	10	1	1	0.35
Mix 15	45	5	50	10	5	15	1	1	0.40
Mix 16	30	-	70	8	4	10	1	1	0.35
Mix 17	30	-	70	10	4	15	1.5	1	0.40
Mix 18	30	-	70	8	4	10	1.5	-	0.45
Mix 19	30	-	70	10	4	10	1	1	0.45
Mix 20	30	-	70	8	4	10	1	1	0.45
Mix 21	30	-	70	8	4	10	1	1	0.50
Mix 22	40	-	60	8	4	-	1	1	0.45
Mix 23	30	-	70	8	4	-	1	1	0.45
Mix 24	20	10	70	8	4	-	1	1	0.45
Mix 25	25	5	70	8	4	-	1	2	0.45
*** Mix 26	25	5	70	1.8	-	-	-	1	0.50
Mix 27	25	5	70	1.6	0.3	0.15	1	1	0.50
Mix 28	25	5	70	2	0.9	0.45	1	1	0.50
Mix 29	25	5	70	1.8	0.6	0.30	1	1	0.49
Mix 30	25	5	70	1.6	0.3	0.15	1	1	0.40

* control sample no.1, ** control sample no.2, *** control sample no.3.

2.2. Sample Preparations

An electric mixer, EX-EM2000 EXTRAMAN 2000W, was used to prepare all mixes. The FA, GGBFS, PCC, K_2CO_3, SRA, CaO, sodium lignosulfonate (SP), and fine aggregates were blended in the mixture for 2 min according to their sample of mix compositions. After that, water was added slowly to the mixtures and continued blending for another 3 min to ensure the mortar paste was uniform. Then, all the fresh mortars were immediately cast into 50 mm × 50 mm × 50 mm cubes for the compressive strength test**,** 40 mm × 40 mm × 160 mm for the flexural strength test, 150 mm × 300 mm diameter cylinder for tensile strength test and modulus of elasticity test, and 75 mm × 75 mm × 280 mm for drying shrinkage measurement. All filled moulds were vibrated for 2 min using a shaking table. The mixtures were demolded after 24 h before being cured in an ambient lab temperature of 29 °C, with relative humidity (RH) of 65% until the testing on days 7, 14, and 28 of curing age. For the compressive strength test, samples were taken out for curing under standard laboratory climate (dry conditioning) for 7 days at 21+/−2 Celsius and 60+/−10% RH.

2.3. Experimental Procedures

To study mechanical strength, hardened mortar's compressive strength and flexure strength were evaluated at 7-d, 14-d, and 28-d curing age. Compression test machine AUTOMAX5 was used at a loading rate of 1000 N/s per the EN12190 test method and a three-point flexure test under a displacement-controlled condition where the load was applied at mid-span in compliance with BS EN 13892-2:2002. The mean value of three readings of each sample produced in triplicate for every test was recorded and taken as their final strength value. In addition, a test on the static modulus of elasticity mortars was conducted at 28-d of age with basic stress of 0.5 N/mm^2, and the stress increased at a constant rate within the range of 0.6 $N/mm^2/s$ until the stress was equal to one-third of the compressive strength of the concrete is reached in compliance with BS 1881. Three cylindrical specimens of 150 mm × 300 mm size for the selected mortar sample formula were prepared, and the average and standard deviation were calculated and reported. Indirect tensile strength was employed using a tensile splitting method on cylindrical mortars for the selected mortar sample and assessed at 28-d of age following ASTM C496 at a loading rate of 1MPa/s. For drying shrinkage measurement, a test was conducted on the prism samples according to BS 1920-8:2009, tested at 28 days of curing age.

3. Result and Discussion

3.1. Compressive Strength

The seven-day compressive strength for 30 samples ranged from 2 N/mm^2 to 23 N/mm^2, as shown in Figures 1–3. Mix 30, composed of 25% FA, 5% GGBFS, and 70% OPC, recorded the highest compressive strength with 23.76 N/mm^2, nearing the minimum strength requirement at 28 days of curing age for structural repair products class R3 of EN1504-3 standard. For the mortar samples, Mix 5, 26, 27, 28, and 29 all recorded compressive strength above 15 N/mm^2 and had the potential to comply with the minimum strength requirement at 28 days of curing age for non-structural repair products class R2 of EN1504-3 standard.

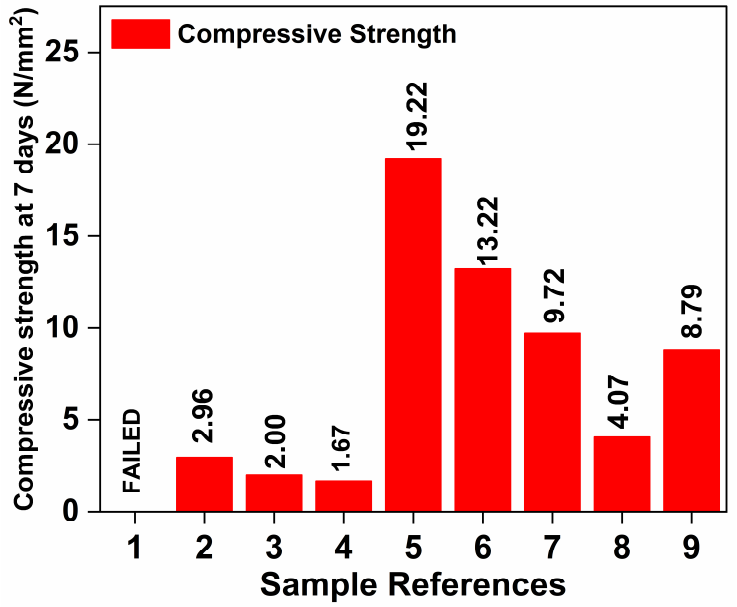

Figure 1. Compressive strength at 7 days of curing age—Stage 1.

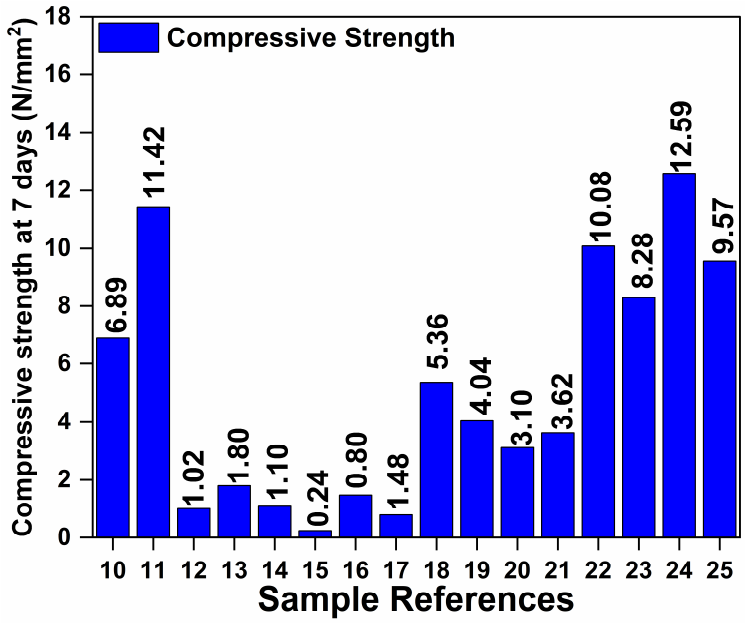

Figure 2. Compressive strength at 7 days of curing age—Stage 2.

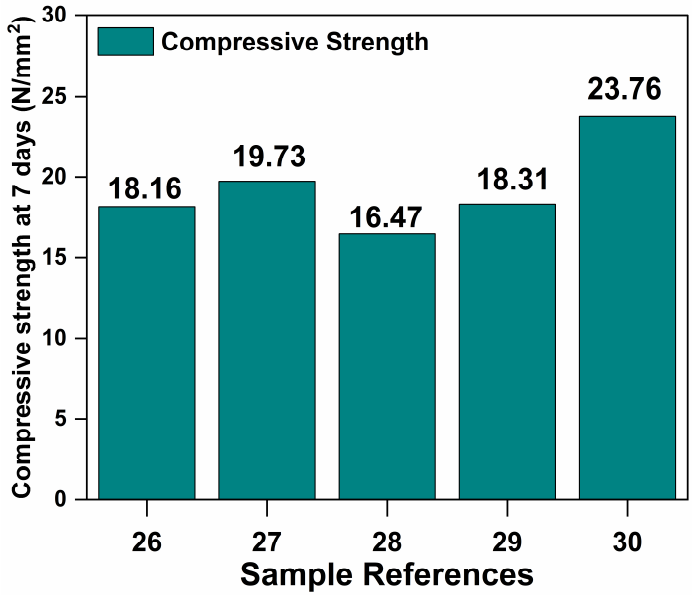

Figure 3. Compressive strength at 7 days of curing age—Stage 3.

Adding FA may slower the strength development of mortar at an early age and clarify the lowest compressive strength reported for samples. Mix 7–13 consisted of 60–80% FA. Without OPC, sample Mix 1 was prepared as a control sample consisting of 85% FA and 15% GGBFS and was activated by a 6% alkali activator, referred to as the first stage of this experiment for mortar samples 1–9 (Figure 1). It was reported that the total aggregate content did not affect the flexural strength development of one-part AAMs [29]. Thus, aggregate-to-binder ratios were set to 3 as a source of calcium and increased the mortar volume for the first three mortar samples, Mix 1–3. However, as observed in these three samples, they were not hardened enough and immediately collapsed when the applied load was placed on the cube samples for testing.

Furthermore, these three samples were activated with a low water-to-binder (W/B) ratio of 0.3, contributing to lower compressive strength. As a result, the cube samples were brittle, sandy, cracked and failed due to insufficient water to initiate the geopolymeratation process. The W/B ratio increased from 0.3 to 0.45 for Mix 3–9 and still only managed to get low compressive strength, except for Mix 5 (W/B ratio of 0.49), which was also designed with an aggregate-to-binder ratio of 1 and lower FA volume (than sample Mix 4) has recorded 13.22 N/mm^2 for seven days of curing age offered important indication on the optimum design of aggregate-to-binder ratio. A higher aggregate-to-binder ratio between 1.5 to 3.0 in this study led to low compressive strength at seven days of curing age because the insufficient hydration of main gel products of C-S-H could not wholly wrap the surface of the fine aggregate, creating more porous structures that make it physically not solid [30].

Mix 10 was designed as a control sample no.2 without admixtures to evaluate the compressive strength trend for mortar samples. Mixes 11–24 were prepared for the second stage (Figure 2) in this compressive strength test experiment. The mortar samples Mix 10 has a 6% alkali activator and W/B ratio of 0.35 and recorded compressive strength of 6.89 N/mm^2. In addition, a 1–10% CaO was added to the mortar because the CaO could supply additional calcium, increase the exothermic level for the hydration process, and react with silica and alumina from FA to produce additional C-S-H and C-A-S-H. Furthermore, the higher silica content in FA increased the dissolution and polymerization process. A higher Si/Al ratio in FA promotes low porosity microstructures, ensuring high sample compactness and enhancing compressive strength [31]. Excessive CaO, however, could lead to strength loss due to the fast chemical reaction of the matrix, subsequently generating unbalanced gel binder structures that affect strength development [32].

Further investigation found that a higher volume of CaO between 10–15% of mix composition was one factor in the poor compressive strength recorded for Mix 12–21. As a result, the volume of FA was reduced to 45% and 40% in Mix 14, 15 and 22 but still showed poor compressive strength. At the same time, samples with 30% FA without GGBFS continued a low compressive strength value trend below 10N/mm^2 as recorded for samples Mix 16–23, which gives a significant indication of the influence of GGBFS and its relation with FA to generate a stronger bond of prominent C-S-H gels.

A higher volume of GGBFS than FA in sample Mix 24 has shown slight improvement for 7-day compressive strength but is still within 50% of the targeted strength of class R3 standard. Nevertheless, it was reported that higher slag content is susceptible to autogenous shrinkage and cracking due to the rapid acceleration of the reactions [14]. Besides that, it was found that without CaO, the 4% SRA-only was inefficient in influencing the compressive strength performance of sample Mix 25. Therefore, based on the compressive strength result at seven days for Mix 10–15 (admixtures effect) and Mix 16–25 (GGBFS effect), Mix 26 was designed as a control sample no.3 for the mix composition consisting of 25% FA and 5% GGBFS with the presence of 70% OPC and 1.8% alkali activator to produce the mortar, subsequently referred as the third stage of the experiment (Figure 3). As a result, the compressive strength result for Mix 26 has an impressive early strength development up to 18N/mm^2 equivalent to 72% of the 28-day minimum compressive strength class R3 and successfully exceeded the 28-day minimum compressive strength for non-structural repair products class R2, both per EN1504-3 specification.

The concentration of alkali activators is crucial for early strength development [26]. A higher alkali activator dosage is required to complete the dissolution of raw materials. At lower alkali activator dosages, the dry mixtures were not fully reacted, causing the mortar to fail to harden at early curing ages. However, for this study, it was shown that a higher percentage negatively affected its mechanical strength, as explained in samples Mix 1–25, which, activated by 6–10% of alkali activators, were unable to react well with precursors and an excessive amount of SRA (1–5%) and CaO (0.5–15%). Therefore, the alkali activator was set between 1.6 and 2.0% for this third test stage. The SRA and CaO were adjusted to 0.3–0.9% of precursor volume for the SRA and 0.15–0.45% for CaO. The W/B ratio was maintained between 0.35–0.5. Moreover, a 1% superplasticizer (SP) and an aggregate-to-binder ratio of 1 were consistently applied to all samples. Therefore, the highest compressive strength value at seven days of age was obtained from sample Mix 30 at an optimum W/B ratio of 0.4, with a sufficient water supply for the geopolymerization process at an early age essential for heat equilibrium, especially with the inclusion of 70% OPC and chemical admixtures (SP, SRA, and CaO) that caused more heat to be released from the exothermic reaction.

Only six samples were selected out of 30 for compressive strength tests at 14 and 28 days of curing age, and the result is recorded in Figure 4. However, compressive strength for samples Mix 26, 27, 28, and 29 deteriorated on day 14 and dropped further toward day 28. It is worthwhile to understand that all mortar samples Mix 26, 27, 28, and 29 have higher water contents with W/B ratios of 0.50 and 0.49 (Mix 29). These findings agreed with [5] on the effect of higher water content reducing the rheology of fresh mortar, subsequently affecting the mechanical strength at the hardened stage. Excessive water content may be caused extra gaps to occur between aggregates, creating voids filled by air when moisture vaporizes. The hardened materials then experience insufficient compaction and become less solid, which affects their strength [33]. Additionally, insufficient alkali cation (Na^+, K^+) to keep the pH raised for the reaction mixtures affects the dissolution process at 28 days of curing age.

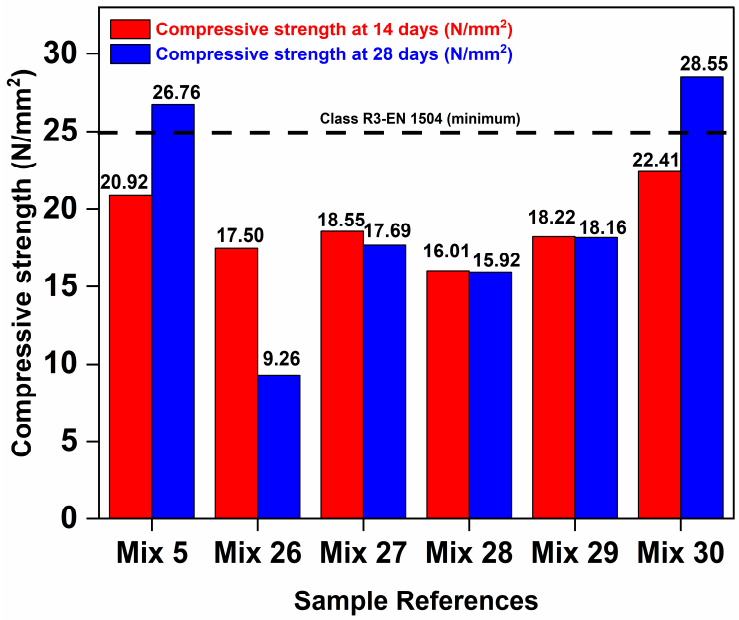

Figure 4. Compressive strength at 14 and 28 days of curing age.

Moreover, Mix 26 as a control sample was composed without admixtures, affecting the stability of the C-A-S-H gels chains and making them prone to chemical attacks. Crack formation due to shrinkage has also lowered the mechanical strength development. The inclusion of a combination of CaO and SRA was reported to control the shrinkage efficiently [21,22]. Still, too much CaO and SRA content in Mix 28 and 29 did not react well with a low dosage of solid alkali activator in addition to higher water content level factors in this report. The reaction rate between precursors and admixtures decreased in low alkali medium, causing low mechanical strength and porous structures [34]. This phenomenon is due to the fact that low pH of carbonate delayed the initial reaction of one-part AAMs and might not be able to fully break down the Al-O and Si-O bonds of the aluminosilicate precursors with the presence of excessive admixtures content. The highest compressive strength recorded at 28 days was 28.55 N/mm² for sample Mix 30, followed by Mix 5, which recorded 26.75 N/mm². These two samples have strength increases over time consistently from seven days to 28 days of curing age, as shown in Figure 5, and exceed the minimum requirement for structural repair product Class R3 of EN1504-3 standard. The microparticle size of powder precursors FA, GGBFS, and OPC in this study exhibit higher specific areas, helpful in improving the reaction for better mechanical strength [6].

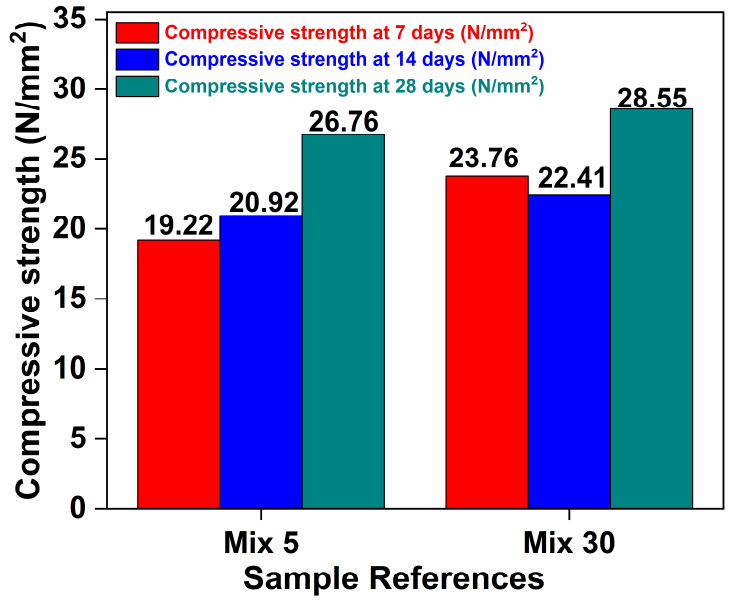

Figure 5. Compressive strength at 7, 14 and 28 days of curing age.

The cracked pattern of the cube samples for sample Mix 30 has little impact on faces in contact with the platens, cone, and shear with fewer macrocracks, generally reflecting its rigidity supporting on higher compressive strength value as shown in Figure 6a. In contrast, Mix 26 experienced an unsatisfactory type of cracked pattern failure, which indicates that it's brittle and not solid, as illustrated in Figure 6b. It was noted that a higher Si/Al ratio for 25% fly ash Class F used in this experiment is physically stable without significant structural disintegration, contributing to the excellent performance in compressive strength [35]. The Si/Al ratio for FA was above 2, within the recommended ratio for higher compressive strength suggested by [31,36,37]. In addition, the main precursors are composed of rich calcium content supplied from GGBFS and OPC sources. Calcium is beneficial for creating C-S-H gels. The combination of FA/GGBFS expands the C-S-H gels chain by creating new C-(A)-S-H co-existing with N-A-S-H gels for excellent mechanical properties [5]. Coppola et al. [38] reported that a one-part alkali-activated mortar activated with a 4% alkali activator recorded compressive strength of 26.4 N/mm² at 28 days of curing age, which is lower than the findings in this study which activated with a minimal dosage of alkali activator.

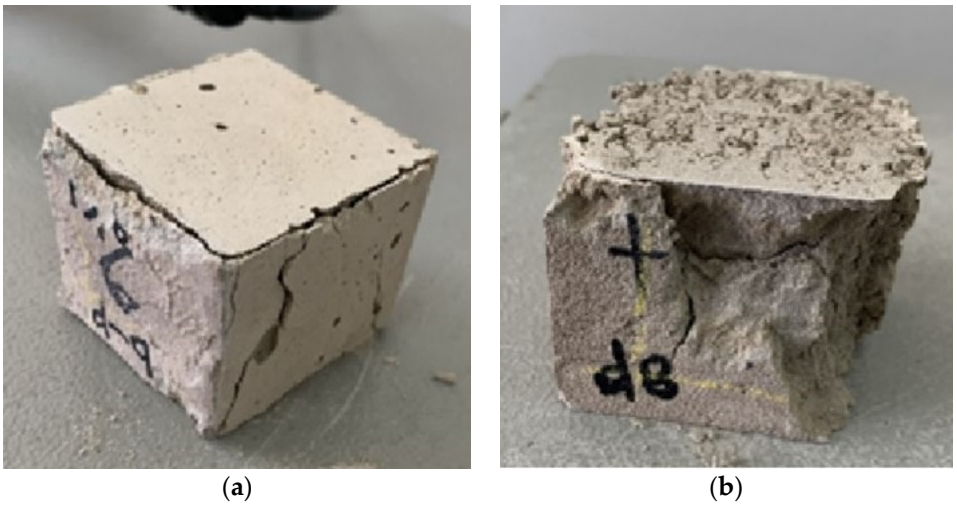

(**a**) (**b**)

Figure 6. (**a**) Cracked pattern failure for mortar sample mix 30 under compressive strength test; (**b**) Cracked pattern failure for mortar sample mix 26 under compressive strength test.

3.2. Flexural Strength

The experiment in this report continues with the flexural test to determine the mechanical compatibility of the mortar and its bending resistance. The test will further explain its tensile strength ability indirectly. Sample Mix 5 and Mix 30 were selected to obtain their flexural strength because their compressive strength at 28 days achieved the minimum requirement as per EN 1504-3 class R3 standard, subsequently referred to as control samples used for the rest of the experiment in this report. At seven, 14 and 28 days, the flexural strength for Mix 30 was 7.4 N/mm^2, 8.05 N/mm^2 and 8.55 N/mm^2, and it was the highest flexural strength recorded between two control mortar samples, as shown in Figure 7, where the flexural strength development increased over time. Both mortar samples recorded above 8 N/mm^2. The addition of 5% GGBFS improved the early mechanical strength of the mortar. At the same time, calcium from FA increased the pozzolanic reaction at the later stage. Besides, a more substantial bonding factor between the binder and the aggregate in the mortar is beneficial for bending resistance behaviour [29].

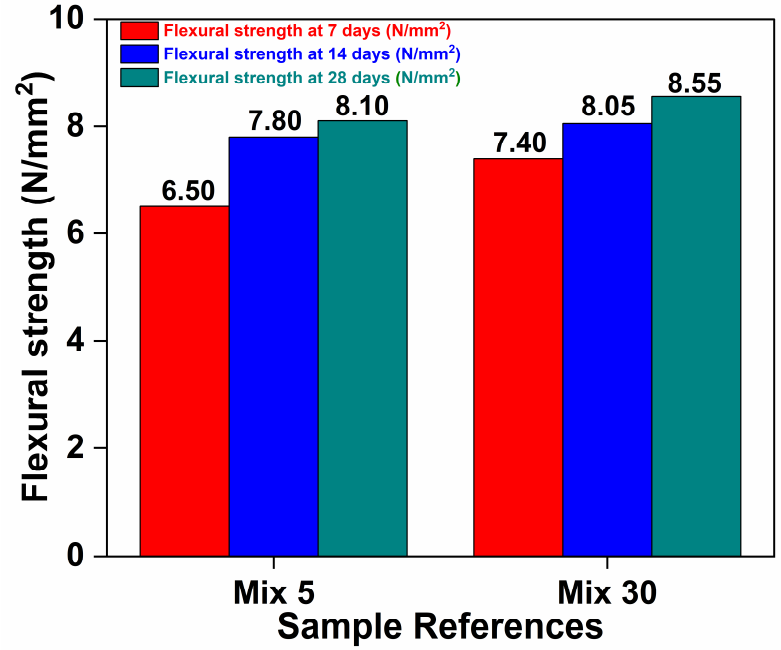

Figure 7. Flexural strength at 7, 14 and 28 days of curing age.

The flexural strength of Mix 30, however, was only around 30% of its compressive strength at 28 days of curing age. This result further explained that the unreinforced mortar cube samples used in this experiment are naturally brittle and very stiff. In addition, the growth of its mechanical strength over time dropped due to microcracks [39]. Nevertheless, the mortar used in the experiment was comparable to the conventional OPC concrete. The concrete standard's flexural strength or modulus of rupture is between 10% and 20% of its compressive strength, depending on the volume and size of the coarse aggregate used in the concrete. Moreover, the 8.55 N/mm^2 flexural strength of Mix 30 exhibited a higher strength value than other one-part alkali-activated materials, as published in past reports [14,21].

3.3. Modulus of Elasticity

Besides the mechanical strength, a higher modulus of elasticity of alkali-activated mortar is essential to offer durable repair materials by providing resistance against elastic deformation when force is applied. The lower aggregate-to-binder ratio reported increased the MOE of concrete activated by one-part AAMs according to [29]. The ratio of

aggregate-to-binder in this experiment was 1, and the mortar samples for the MOE test were cured with water and ambient conditions.

As shown in Table 3, the modulus of elasticity of sample Mix 30 was recorded at 19.6 GPa, and Mix 5 has 18.10 GPa MOE, both complying with the minimum elastic modulus requirement for class R3-EN1504 standard, slightly higher than the modulus of elasticity for most of the two-part alkali-activated mortar, which has been recorded between 15–18 GPa [39,40]. Additionally, they did not require higher temperatures than the two-part AAMs [7]. However, similar to the flexural strength development, the presence of micro-cracks has affected the MOE of one part of alkali-activated mortar [41]. In addition, it is worthing to note that repair materials and substrates may have different moduli of elasticity. For example, concrete substrates generally have an elastic modulus between 30 to 50 GPa. A lower modulus of elasticity of repair material than the substrates has more resilient elements that can take up more force and return to its initial structure [28], subsequently protecting mortar from cracking, thus providing better structural compatibility between the repair mortar and the existing concrete substrates [39].

Table 3. Modulus of Elasticity (MOE) at 28-day of age.

Sample References	Modulus of Elasticity (GPa)
Mix 5	18.10
Mix 30	19.60

3.4. Tensile Strength

The higher aggregate content would increase the splitting tensile strength, and the strength developed over time follows a similar trend with compressive and flexural strength. However, the tensile strength after 28 days was lower than the mixtures with lower aggregate content reported by [29]. The highest splitting tensile strength between these two samples is Mix 30, which recorded 2.05 MPa, equivalent to 10% of its compressive strength at 28 days of curing age, as shown in Table 4, giving a good signal of its bond strength ability to achieve minimum adherence strength 2.0 MPa of class R4, EN1504-3 [42]. Nevertheless, Mix 30 with 2.05 MPa tensile strength was within the range of tensile strength for typical plain cementitious mortar, as reported by [43]. It turns out that the incorporation of slag as a replacement for fly ash for mortar Mix 30 enhanced splitting tensile strength, as reported by [44]. It is worth noting that mortar is good in compression but weak in tension, like typical concrete. The interface transition zone (ITZ) is the weakest link in the hardened mortar, as observed from its microstructure. When a compressive load is applied, the ITZ bridges the load from one aggregate to another in the mortar. On the contrary, the outer surface of aggregates will break from each other when tensile stresses are applied to leave the ITZ to absorb all forces and cause failure.

Table 4. Splitting tensile strength at 28 days of curing age.

Sample References	Splitting Tensile Strength (MPa)
Mix 5	1.80
Mix 30	2.05

3.5. Drying Shrinkage

Shrinkage is one of the significant problems for alkali-activated materials, mainly caused by alkali activator involvement in accelerating the reaction. Jixiang et al. [6] reported that a higher sodium silicate and slag content dosage in alkali-activated materials increased shrinkage. In this report, a lower dosage of alkali activator and slag for the one-part mortar Mix 30 has a length change measured of 260 microstrains at 28 days, while mortar sample Mix 5 documented 350 microstrains. Both recorded less than 400 microstrains under ASTM C157 specification for drying shrinkage measurement as shown

in Table 5, which is much better than the shrinkage level of the two-part alkali-activated materials counterpart. This result also agreed with [45] on the beneficial effect of the shrinkage-reducing admixtures (SRA) in alkali-activated materials. The SRA admixture will limit the tensile stress stimulated by restrained **s**hrinkage, thus avoiding the mortar from early cracks. Therefore, drying shrinkage measurement can indicate the mortar's ability to resist early crack formation and shrinkage-restraining stresses.

Table 5. Drying Shrinkage Measurement at 28 days of curing age.

Sample References	Drying Shrinkage Measurement (Microstrain)
Mix 5	350
Mix 30	260

On the other hand, the low water-to-binder ratio increased the mechanical strength of hardened mortar. Still, it could result in autogenous **s**hrinkage and cracking, affecting the flexural strength over time. Sample Mix 30 mortar in this experiment has proved that even though it was composed of a lower water-to-binder ratio and a lower dosage of alkali activator yet recorded a lower level of drying shrinkage measurement within a maximum of 400 microstrains allowed. The result is also in agreement with [21,22], where the usage of shrinkage-reducing admixtures (SRA) and calcium oxide (CaO) as an expensive agent could reduce the shrinkage level of mortar. It is beneficial to determine CaO dosage in this experiment because the excessive level of calcium may precipitate as gypsum and expand, possibly damaging the mortar's physical structures. However, with an appropriate ratio, the gypsum may also block pores and minimize early corrosion attacks [46]. Furthermore, CaO is an expansive agent that induces a high exothermic reaction when it reacts with water to form a larger volume of hydrated lime particles, which helps the mortar to expand instead of shrinking and only stops expanding at the end of the curing process [22].

Other than that, the applied aggregate-to-binder of 1 for Mix 30 contributed to a better performance of tensile strength where it controlled the shrinkage level where the fine aggregate served as reinforcement to compact and stabilize the materials [42]. It is worth noting that a higher percentage volume of all three admixtures created unbalanced gel structures and affected mechanical strength growth at the early and later stages of the hardening phase, as observed in all 30 mortar samples' compressive strength results in this study. Contrary to the conventional one-part alkali-activated mortar productions, the inclusion of admixtures and OPC reacted well with a low dosage of non-hygroscopic alkali activator, offering cheaper and safer construction products. This type of hybrid one-part AAMs has impressive mechanical strength and a low drying shrinkage level comparable to the conventional OPC mortar and the two-part AAMs mortar counterparts.

4. Conclusions

This study investigated the mechanical strength performance of one-part alkali-activated mortar for concrete structural repair application. The mortar was composed with different mixed design compositions. As a result, mortar sample Mix 30 has the best mechanical strength performance out of 30 different mix design ratios, followed by mortar sample Mix 5. In Mix 30, the OPC binder content was replaced with 30% by-product precursors consisting of 25% class-F fly ash and 5% slag from the GGBFS source. Interestingly, dry mixed precursors were activated with only 1.8% powdered alkaline activator of Potassium carbonate (K_2CO_3). As a result, mortar samples Mix 30 has a water-to-binder ratio of 0.40 compared to Mix 5 activated with a W/B of 0.49. The mechanical strength results for mortar sample Mix 30 complied with the minimum requirements for the compressive strength and modulus of elasticity (MOE) as per the Class R3-EN1504 standard for structural concrete repair materials and successfully achieved the aim of this study.

For one-part AAMs activated with low alkali activator dosage, a single aluminosilicate precursor will not be sufficient to produce the higher compressive strength of mortar.

Combining two or three industrial by-product precursors with OPC demonstrates improved physical structures and mechanical strength. The combination of FA and GGBFS reacted well with the OPC under a low alkaline environment and exhibited acceptable mechanical strength performances. The flexural and splitting tensile strengths result for Mix 30 showed that the mortar has higher bending resistance and can resist the applied stress as a sign of solid bonding strength between mortar and concrete substrates, subsequently promoting its potential to be applied for concrete structural repair applications. Nevertheless, lower MOE of repair mortar than the concrete substrate is essential to ensure combability between two bonding materials to resist force while maintaining the bond at interface transition zone (ITZ).

The combination of three powder admixtures enhances the mechanical properties of the mortar compared to samples without admixtures. Using SRA and CaO reduced the internal stress, controlled the expansion of the mortar, and ensured reliable mechanical strength progress. Adding a superplasticizer (SP) lengthens the setting time and controls the hydration process rates.

Future studies will focus on the rheology behaviour of the fresh mortar using this new mix design formulation to ensure its consistency and flexibility adopted for in-situ application. In addition, improved workability of mortar will offer better mechanical strength, beneficial for the pull-off bond strength performance between the repair mortar and concrete substrate for concrete patching applications as part of concrete repair techniques.

Author Contributions: Conceptualization, E.Y.; Data curation, E.Y.; Formal analysis, E.Y.; Funding acquisition, E.Y.; Investigation, E.Y.; Methodology, E.Y.; Project administration, E.Y. and S.B.; Supervision, S.B.; Visualization, S.B.; Writing—original draft, E.Y. All authors have read and agreed to the published version of the manuscript.

Funding: This research received no external funding.

Institutional Review Board Statement: Not applicable.

Informed Consent Statement: Not applicable.

Data Availability Statement: Not applicable.

Acknowledgments: Special thanks to Makmal Kerja Raya Malaysia (MKRM), Engineering New Zealand, The Association of German Engineers (VDI) and the Public Service Department, Sabah (JPANS), Malaysia, for contributing to the outcome of this experiment.

Conflicts of Interest: The authors declare no conflict of interest.

References

1. Ren, J.; Sun, H.; Li, Q.; Li, Z.; Ling, L.; Zhang, X.; Wang, Y.; Xing, F. Experimental comparisons between one-part and normal (two-part) alkali-activated slag binders. *Constr. Build. Mater.* **2021**, *309*, 125177. https://doi.org/10.1016/j.conbuildmat.2021.125177.
2. Peng, M.X.; Wang, Z.H.; Shen, S.H.; Xiao, Q.G.; Li, L.J.; Tang, Y.C.; Hu, L.L. Alkali fusion of bentonite to synthesize one-part geopolymeric cements cured at elevated temperature by comparison with two-part ones. *Constr. Build. Mater.* **2017**, *130*, 103–112. https://doi.org/10.1016/j.conbuildmat.2016.11.010.
3. Xu, G.; Shi, X. Characteristics and applications of fly ash as a sustainable construction material: A state-of-the-art review. *Resour. Conserv. Recycl.* **2018**, *136*, 95–109. https://doi.org/10.1016/j.resconrec.2018.04.010.
4. Ding, Y.-C.; Cheng, T.-W.; Dai, Y.-S. Application of geopolymer paste for concrete repair. *Struct. Concr.* **2017**, *18*, 561–570. https://doi.org/10.1002/suco.201600161.
5. Phoo-Ngernkham, T.; Hanjitsuwan, S.; Li, L.-Y.; Damrongwiriyanupap, N.; Chindaprasirt, P. Adhesion characterization of Portland cement concrete and alkali-activated binders. *Adv. Cem. Res.* **2019**, *31*, 69–79. https://doi.org/10.1680/jadcr.17.00122.
6. Wang, J.; Huang, T.; Cheng, G.; Liu, Z.; Li, S.; Wang, D. Effects of fly ash on the properties and microstructure of alkali-activated FA/BFS repairing mortar. *Fuel* **2019**, *256*, 115919. https://doi.org/10.1016/j.fuel.2019.115919.
7. Adesanya, E.; Ohenoja, K.; Di Maria, A.; Kinnunen, P.; Illikainen, M. Alternative alkali-activator from steel-making waste for one-part alkali-activated slag. *J. Clean. Prod.* **2020**, *274*, 123020. https://doi.org/10.1016/j.jclepro.2020.123020.

8. Shah, S.F.A.; Chen, B.; Oderji, S.Y.; Haque, M.A.; Ahmad, M.R. Comparative study on the effect of fiber type and content on the performance of one-part alkali-activated mortar. *Constr. Build. Mater.* **2020**, *243*, 11822. https://doi.org/10.1016/j.conbuildmat.2020.118221.
9. Luukkonen, T.; Abdollahnejad, Z.; Yliniemi, J.; Kinnunen, P.; Illikainen, M. Comparison of alkali and silica sources in one-part alkali-activated blast furnace slag mortar. *J. Clean. Prod.* **2018**, *187*, 171–179. https://doi.org/10.1016/j.jclepro.2018.03.202.
10. Kadhim, A.; Sadique, M.; Al-Mufti, R.; Hashim, K. Developing one-part alkali-activated metakaolin/natural pozzolan binders using lime waste. *Adv. Cem. Res.* **2021**, *33*, 342–356. https://doi.org/10.1680/jadcr.19.00118.
11. Li, L.; Lu, J.-X.; Zhang, B.; Poon, C.-S. Rheology behavior of one-part alkali activated slag/glass powder (AASG) pastes. *Constr. Build. Mater.* **2020**, *258*, 120381. https://doi.org/10.1016/j.conbuildmat.2020.120381.
12. Abdollahnejad, Z.; Mastali, M.; Falah, M.; Shaad, K.M.; Luukkonen, T.; Illikainen, M. Durability of the Reinforced One-Part Alkali-Activated Slag Mortars with Different Fibers. *Waste Biomass Valorization* **2020**, *12*, 487–501. https://doi.org/10.1007/s12649-020-00958-x.
13. Oderji, S.Y.; Chen, B.; Ahmad, M.R.; Shah, S.F.A. Fresh and hardened properties of one-part fly ash-based geopolymer binders cured at room temperature: Effect of slag and alkali activators. *J. Clean. Prod.* **2019**, *225*, 1–10. https://doi.org/10.1016/j.jclepro.2019.03.290.
14. Shah, S.F.A.; Chen, B.; Oderji, S.Y.; Haque, M.A.; Ahmad, M.R. Improvement of early strength of fly ash-slag based one-part alkali activated mortar. *Constr. Build. Mater.* **2020**, *246*, 118533. https://doi.org/10.1016/j.conbuildmat.2020.118533.
15. Kramar, S.; Šajna, A.; Ducman, V. Assessment of alkali activated mortars based on different precursors with regard to their suitability for concrete repair. *Constr. Build. Mater.* **2016**, *124*, 937–944. https://doi.org/10.1016/j.conbuildmat.2016.08.018.
16. Abdollahnejad, Z.; Mastali, M.; Luukkonen, T.; Kinnunen, P.; Illikainen, M. Fiber-reinforced one-part alkali-activated slag/ceramic binders. *Ceram. Int.* **2018**, *44*, 8963–8976. https://doi.org/10.1016/j.ceramint.2018.02.097.
17. Alzaza, A.; Ohenoja, K.; Illikainen, M. Enhancing the mechanical and durability properties of subzero-cured one-part alkali-activated blast furnace slag mortar by using submicron metallurgical residue as an additive. *Cem. Concr. Compos.* **2021**, *122*, 104128. https://doi.org/10.1016/j.cemconcomp.2021.104128.
18. Alzaza, A.; Ohenoja, K.; Illikainen, M. Mechanical properties of ambient cured one-part hybrid OPC-geopolymer concrete. *Constr. Build. Mater.* **2018**, *186*, 330–337. https://doi.org/10.1016/j.conbuildmat.2018.07.160.
19. Alzaza, A.; Ohenoja, K.; Illikainen, M. Microstructure and macro properties of sustainable alkali-activated fly ash mortar with various construction waste fines as binder replacement up to 100%. *Cem. Concr. Compos.* **2022**, *134*, 104733. https://doi.org/10.1016/j.cemconcomp.2022.104733.
20. Liu, M.; Wang, C.; Wu, H.; Yang, D.; Ma, Z. Reusing recycled powder as an eco-friendly binder for sustainable GGBS-based geopolymer considering the effects of recycled powder type and replacement rate. *J. Clean. Prod.* **2022**, *364*, 132656. https://doi.org/10.1016/j.jclepro.2022.132656.
21. Liu, M.; Wang, C.; Wu, H.; Yang, D.; Ma, Z. The combined use of admixtures for shrinkage reduction in one-part alkali activated slag-based mortars and pastes. *Constr. Build. Mater.* **2020**, *248*, 118682. https://doi.org/10.1016/j.conbuildmat.2020.118682.
22. Ngassam, I.L.T.; Arito, P.; Beushausen, H. A new approach for the mix design of (patch) repair mortars. *African J. Sci. Technol. Innov. Dev.* **2018**, *10*, 259–265. https://doi.org/10.1080/20421338.2018.1452845.
23. Ngassam, I.L.T.; Arito, P.; Beushausen, H. One-part alkali-activated binder produced from inertized asbestos cement waste. *J. Clean. Prod.* **2022**, *367*, 132966. https://doi.org/10.1016/j.jclepro.2022.132966.
24. Huseien, G.F.; Mirza, J.; Ismail, M.; Ghoshal, S.; Hussein, A.A. Geopolymer mortars as sustainable repair material: A comprehensive review. *Renew. Sustain. Energy Rev.* **2017**, *80*, 54–74. https://doi.org/10.1016/j.rser.2017.05.076.
25. Yin, K.; Jiang, Y.; He, H.; Ren, J.; Li, Z. Characterization of one-part alkali-activated slag with rice straw ash. *Constr. Build. Mater.* **2022**, *345*, 128403. https://doi.org/10.1016/j.conbuildmat.2022.128403.
26. Liu, C.; Yao, X.; Zhang, W. Controlling the setting times of one-part alkali-activated slag by using honeycomb ceramics as carrier of sodium silicate activator. *Constr. Build. Mater.* **2020**, *235*, 117091. https://doi.org/10.1016/j.conbuildmat.2019.117091.
27. Luukkonen, T.; Abdollahnejad, Z.; Ohenoja, K.; Kinnunen, P.; Illikainen, M. Suitability of commercial superplasticizers for one-part alkali-activated blast-furnace slag mortar. *J. Sustain. Cem. Mater.* **2019**, *8*, 244–257. https://doi.org/10.1080/21650373.2019.1625827.
28. Teixeira, O.G.; Geraldo, R.H.; da Silva, F.G.; Gonçalves, J.P.; Camarini, G. Mortar type influence on mechanical performance of repaired reinforced concrete beams. *Constr. Build. Mater.* **2019**, *217*, 372–383. https://doi.org/10.1016/j.conbuildmat.2019.05.035.
29. Haruna, S.; Mohammed, B.S.; Wahab, M.; Liew, M. Effect of paste aggregate ratio and curing methods on the performance of one-part alkali-activated concrete. *Constr. Build. Mater.* **2020**, *261*, 120024. https://doi.org/10.1016/j.conbuildmat.2020.120024.
30. Zhang, S.; He, Y.; Zhang, H.; Chen, J.; Liu, L. Effect of fine sand powder on the rheological properties of one-part alkali-activated slag semi-flexible pavement grouting materials. *Constr. Build. Mater.* **2022**, *333*, 127328. https://doi.org/10.1016/j.conbuildmat.2022.127328.
31. Qureshi, M.N.; Ghosh, S. Effect of Si/Al ratio on engineering properties of alkali-activated GGBS pastes. *Green Mater.* **2014**, *2*, 123–131. https://doi.org/10.1680/gmat.14.00001.
32. Phoo-Ngernkham, T.; Phiangphimai, C.; Intarabut, D.; Hanjitsuwan, S.; Damrongwiriyanupap, N.; Li, L.-Y.; Chindaprasirt, P. Low cost and sustainable repair material made from alkali-activated high-calcium fly ash with calcium carbide residue. *Constr. Build. Mater.* **2020**, *247*, 118543. https://doi.org/10.1016/j.conbuildmat.2020.118543.

33. Panda, S.; Sarkar, P.; Davis, R. Effect of Water-Cement Ratio on Mix Design and Mechanical Strength of Copper Slag Aggregate Concrete. *IOP Conf. Ser. Mater. Sci. Eng.* **2020**, *936*, 012019. https://doi.org/10.1088/1757-899x/936/1/012019.
34. Askarian, M.; Tao, Z.; Samali, B.; Adam, G.; Shuaibu, R. Mix composition and characterization of one-part geopolymers with different activators. *Constr. Build. Mater.* **2019**, *225*, 526–537. https://doi.org/10.1016/j.conbuildmat.2019.07.083.
35. Thokchom, S.; Mandal, K.K.; Ghosh, S. Effect of Si/Al Ratio on Performance of Fly Ash Geopolymers at Elevated Temperature. *Arab. J. Sci. Eng.* **2012**, *37*, 977–989. https://doi.org/10.1007/s13369-012-0230-5.
36. Lau, C.K.; Rowles, M.R.; Parnham, G.N.; Htut, T.; Ng, T.S. Investigation of geopolymers containing fly ash and ground-granulated blast-furnace slag blended by amorphous ratios. *Constr. Build. Mater.* **2019**, *222*, 731–737. https://doi.org/10.1016/j.conbuildmat.2019.06.198.
37. Wang, Y.; Liu, X.; Zhang, W.; Li, Z.; Zhang, Y.; Li, Y.; Ren, Y. Effects of Si/Al ratio on the efflorescence and properties of fly ash based geopolymer. *J. Clean. Prod.* **2020**, *244*, 118852. https://doi.org/10.1016/j.jclepro.2019.118852.
38. Coppola, L.; Coffetti, D.; Crotti, E. Pre-packed alkali activated cement-free mortars for the repair of existing masonry buildings and concrete structures. *Constr. Build. Mater.* **2018**, *173*, 111–117. https://doi.org/10.1016/j.conbuildmat.2018.04.034.
39. Nunes, V.A.; Borges, P.H.; Zanotti, C. Mechanical compatibility and adhesion between alkali-activated repair mortars and Portland cement concrete substrate. *Constr. Build. Mater.* **2019**, *215*, 569–581. https://doi.org/10.1016/j.conbuildmat.2019.04.189.
40. Huseien, G.F.; Shah, K.W. Performance evaluation of alkali-activated mortars containing industrial wastes as surface repair materials. *J. Build. Eng.* **2020**, *30*, 101234. https://doi.org/10.1016/j.jobe.2020.101234.
41. Coppola, L.; Coffetti, D.; Crotti, E.; Gazzaniga, G.; Pastore, T. The durability of one-part alkali-activated slag-based mortars in different environments. *Sustainability* **2020**, *12*, 3561. https://doi.org/10.3390/su12093561.
42. Salazar, R.A.R.; Jesús, C.; de Gutiérrez, R.M.; Pacheco-Torgal, F. Alkali-activated binary mortar based on natural volcanic pozzolan for repair applications. *J. Build. Eng.* **2019**, *25*, 100785. https://doi.org/10.1016/j.jobe.2019.100785.
43. Wazien, A.W.; Abdullah, M.M.A.B.; Razak, R.A.; Rozainy, M.M.R.; Tahir, M.F.M.; Hussin, K. Potential of geopolymer mortar as concrete repairing materials. *Mater. Sci. Forum* **2016**, *857*, 382–387. https://doi.org/10.4028/www.scientific.net/MSF.857.382.
44. Huseien, G.; Ismail, M.; Tahir, M.; Mirza, J.; Hussein, A.; Khalid, N.; Sarbini, N. Performance of sustainable alkali-activated mortars containing solid waste ceramic powder. *Chem. Eng. Trans.* **2018**, *63*, 673–678. https://doi.org/10.3303/cet1863113.
45. Coppola, L.; Coffetti, D.; Crotti, E.; Marini, A.; Passoni, C.; Pastore, T. Lightweight cement-free alkali-activated slag plaster for the structural retrofit and energy upgrading of poor quality masonry walls. *Cem. Concr. Compos.* **2019**, *104*, 103341. https://doi.org/10.1016/j.cemconcomp.2019.103341.
46. Sturm, P.; Gluth, G.; Jäger, C.; Brouwers, H.; Kühne, H.-C. Sulfuric acid resistance of one-part alkali-activated mortars. *Cem. Concr. Res.* **2018**, *109*, 54–63. https://doi.org/10.1016/j.cemconres.2018.04.009.